WINDING PROCESS MODELLING – VALIDATION THROUGH SPRING-IN PREDICTION

Patrick Pérès[1], Jean Marc Dupillier[2], Corey Lynam[3] and Alireza Forghani[4]

[1] Airbus Safran Launchers, av Général NIOX, BP20011, 33165 St Médard en Jalles, France, patrick.peres@airbusafran-launchers.com
[2] Airbus Safran Launchers, av Général NIOX, BP20011, 33165 St Médard en Jalles, France, jean-marc.dupillier@airbusafran-launchers.com
[3] Convergent Manufacturing Technologies Inc, 6190 Agronomy Rd, Suite 403 Vancouver BC V6T 1Z3, Canada, Corey.Lynam@convergent.ca, http://www.convergent.ca
[4] Convergent Manufacturing Technologies Inc, 6190 Agronomy Rd, Suite 403 Vancouver BC V6T 1Z3, Canada, Alireza.Forghani@convergent.ca, http://www.convergent.ca

Keywords: Modelling, Winding, Residual stress, Spring-in

ABSTRACT

Even if many studies have been performed to model winding process, difficulties are still encountered to well predict the residual stresses. The compaction of the composite is governed by the tension of the tow and by the thermal expansion of the mandrel. Therefore this specific process generates a gradient of fiber volume fraction throughout the composite thickness. Hence, performance of high pressure vessel strongly depends on this gradient of volume fraction and hence to fiber tension. Fiber de-tensioning caused by resin flow can generate wrinkling and weaving which significantly reduce the performance of the vessel.

This paper presents complementary improvement brought to the classical theory in order to better take into account material artifacts as weaving and internal voids. Comparison between experimental measure as pressure, spring-in effect and numerical simulation has allowed concluding this approach is rather effective to better predict the influence of winding tension and mandrel thermal properties.

1 INTRODUCTION

From an engineering point of view, process modelling can allow to better master material health (porosity, weaving, fiber volume fraction, degree of cure), control piece distortion (problem of assembly, to avoid machining), minimize residual stresses.

Prediction of distortion of composite structures which is linked to minimizing residual stresses is not a new topic and several scientific papers have been publishing for more than 30 years now [1-3]. Application of academic studies to real structures is complex when the process addresses multi-physical problems for which a long phase of validation is needed.

We have learnt from literature that in general, the major contributors of composite distortion are thermal expansion, cure shrinkage, laminate lay-up, cure temperature and mold thermal expansion [4]. The specificity of the winding process implies to take into account the contribution of the lay-up sequence, winding tension, winding-tension gradient, winding time, the interaction between winding tension and winding time and the pressure generated by the mandrel in composite compaction which all affects composite strength. Moreover there is a strong correlation between fiber volume fraction in the hoop layers and the failure pressure.

In the industry, engineers are keeping in mind that benefits of Manufacturing Process Simulation are mainly measured when they:

-reduce cost for process developments
-reduce cost of manufactured parts
-reduce cycle time.

2 CHOICE OF THE TEST SAMPLE WITH ITS INSTRUMENTATION

Validation of the multi-physic models has been guided by manufacturing simple samples with are representative to the conditions used for high pressure vessel manufacturing. The second key driver was to access to relevant measures which will be performed during all phases from winding to demolding after curing. Finally it has been chosen to manufacture $[90]_{20}$ rings of 300mm inner diameter and with twenty circumferential layers of carbon tow (IM fibre) pre-impregnated with epoxy resin (Fig. 1). All conditions of tow deposition on the mandrel are similar to the high pressure vessel manufactured in the workshop in terms of tow size, tow tension, winding speed and time between end of winding and curing.

Reliability of the instrumentation is the key issue to validate models. If temperature measurement can be achieved rather easily, stress-strain measure is more complex. Specific embedded sensors have to be used in order to not modify the real state/condition. Strain measurement with Optical fiber (Bragg or Rayleigh principle) is the best method. Another pertinent parameter is the pressure measurement because it is linked to hoop stresses [5]. Thanks to very thin sensors available on market (Flexiforce, thickness 0,208mm and sensing aera of 9,53mm in diameter), pressure measure can be recorded onto the mandrel and even in between two layers. Finally the easiest meyhod to validate the simulation is to measure the residual deformation due to the relaxation residual stresses inherent to any composite structure manufacturing. Residual deformation is measured when ring is transversally cut. Release of residual stresses generates here spring-in (closure of the ring) of $[90]_{20}$ ring (Fig. 1).

Moreover, knowledge of the thickness of the ring after curing and the gradient of fiber volume fraction inside the ring are valuable information to strengthen the pertinence of the models.

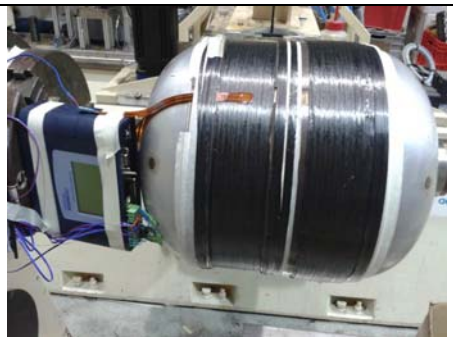

Ring manufacturing with pressure sensor instrumentation

Illustration of spring-in effects

Figure 1: $[90]_{20}$ ring manufacturing

3 STUDY OF THE INFLUENCE OF PROCESS PARAMETER

Maximum fiber volume fraction and gradient of fiber volume are strongly affected by winding tension and winding time. In principle high winding tension and shorter winding time produce higher fiber volume. Fiber volume is related to fiber motion through the resin thanks to tension and to resin viscosity and fiber bed permeability. This mechanism of fiber motion is also related to mandrel expansion during curing phase until gelation threshold of the resin is reached.

Therefore our study has been focusing in studying two process parameters; winding tension and mandrel thermal expansion.

4 SIMULATION OF THE WINDIG PHASE

4.1 Theory

During winding stage, resin is in pre-gelation state and viscous flow is the dominant mechanism for movement of resin. The model based on porous material (fiberbed) with resin (Darcy law) is used to

describe the behavior of the material during winding state and the pre gelation state [6, 7]. COMPRO's Flow-Compaction simulation framework is employed to model the winding process.

$$\phi\left(\frac{1}{K_r}\frac{\partial p}{\partial t} - 3.CTE_r\frac{\partial T}{\partial t} + 3.CCS_r\frac{\partial X}{\partial t}\right) + \nabla.(\dot{u}_f - \frac{K}{\mu}\nabla p) = 0 \quad (1)$$

ϕ Volume fraction of resin
$\dot{u}_f$ Local speed motion of the fiber bed
T Temperature
X Crosslinking (polymerization rate)
p Resin pressure
CTE_r, CCS_r : thermal expansion and thermal shrinkage of the resin.
Note: CTEr, CCSr are ignored during winding stage.
C : compliance matrix of the fiberbed
K_r : compressibility modulus of the resin

In this stage applied load is shared between fiberbed and viscous resin. The effective stress (σ_{eff}) is written with a combination of compliance matrix of fiberbed (C) and resin pressure (p).

$$\dot{\boldsymbol{\sigma}}_{eff} = \mathbf{C} : \dot{\boldsymbol{\varepsilon}} - \dot{p}\mathbf{I} \quad (2)$$

Table 1 synthetizes the overall properties required for winding process simulation and the associated test methods.

Thermo-chemical analysis	Flow-Compaction Analysis	Fiberbed elastic properties
-Degree of cure (DSC) -Heat of reaction (DSC) -Glass transition (DSC) -Density -Specific heat capacity (deduced from modulated DSC) -Thermal conductivity	-Initial fibre volume fraction -Resin permeability *Theory :Carman-Kozeny (longitudinal mode) and Gutowski (transverse mode)* -Fibre bed compaction *See Fig. 2* -Resin viscosity	-Elastic-viscoelastic constants -Coefficient of thermal expansion (CTE) -Cure shrinkage *These properties are determined with DMA tests*

Table 1: Material properties used for the simulation

Based on three-point bending technique developed at Convergent, several bi-material beam samples composed of UD composite and a steel shim were prepared and cured under isothermal conditions. Their mid-span deflection was measured at low frequency with Dynamic Mechanical Analysis device. Resin properties as modulus, thermal expansion and cure shrinkage are then determined from these tests. Through-thickness response of the fiberbed follows a compaction curve shown in Fig. 2.

The dominant consolidation mechanism during winding stage is the collapse of gaps and bleed of resin into the inter-tow gaps. The mechanism of resin flow in radial direction is not systematically observed during the winding phase. In fact we can observe internal gaps, towpreg overlapping and voids where resin can flow into. We cannot assume perfectly straight fibers with full stiffness in the fiber directions (see Fig. 3).

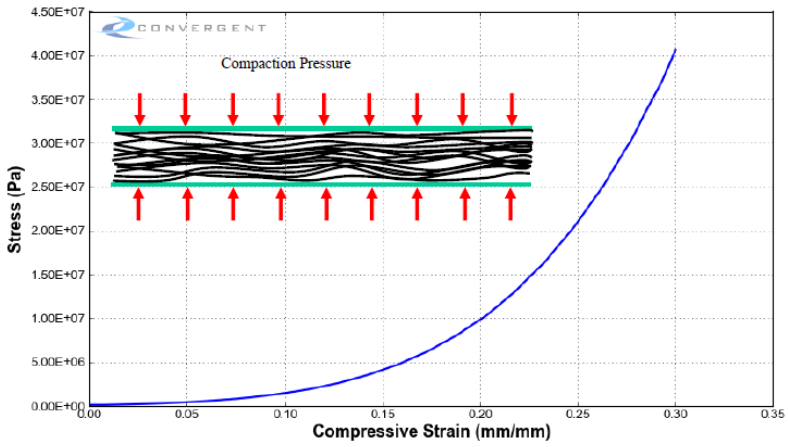

Figure 2: Through the thickness fiberbed compaction curve

Compaction close to the mandrel

Compaction inside the ring

Figure 3: Illustration of artifacts (voids, overlaps, weaving) observed in some $[90]_{20}$ rings.

To include the effect of internal voids in the simulations, resin rich interlayer elements were added to the finite element mesh. Resin was allowed to bleed out of the middle of these interlayer elements (Fig. 4).

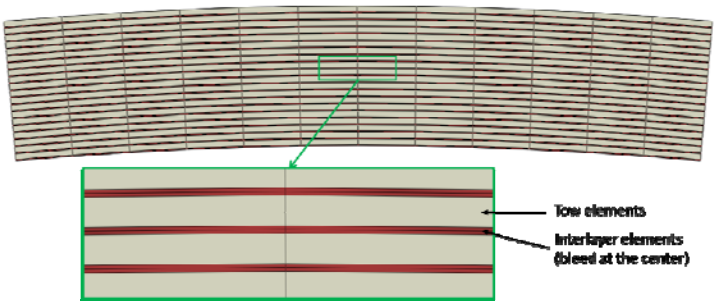

Figure 4: Part mesh with resin rich interlayer elements that bleed in their middle

To capture the effect of fiber waviness in the simulation, a viscoelastic hardening model is applied to the in-plane fiberbed properties (see Fig. 5). The elastic component is a hardening spring which represents stiffening of the fibers as a function of applied tensile strain. The viscoelastic component represents the reduction of axial modulus due to relaxation of the lateral supports when the wavy tow is heated up. Relaxation timescales are chosen to be proportional to resin viscosity.

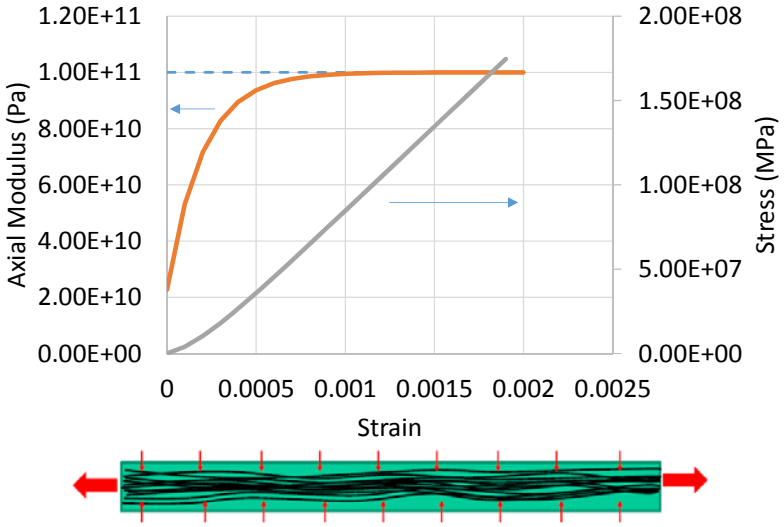

Figure 5: Viscoelastic hardening behavior applied to tow direction of fiberbed

4.2 Comparison between simulation and experimental results

The first step of the simulation was to reproduce the evolution of the contact pressure during winding where pressure relaxation is observed. This relaxation depends on resin viscosity and permeability of the layers which govern resin flow out. Fig 6 illustrates the measured and predicted pressures on the surface of mandrel during winding process. This figure shows a good agreement between the trends measured and predicted by the model. As shown in this figure maximum pressure is reached before the 10th layer deposition independently of winding tension. On the other hand, the maximum pressure level depends on winding tension (proportional in this case). Similar observations were reported by H T Hahn [8].

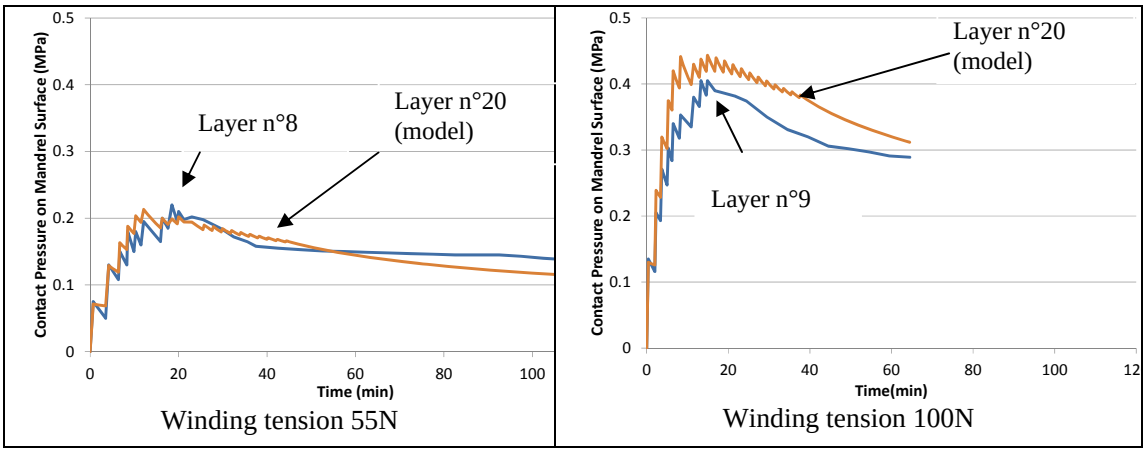

Figure 6: Comparison simulation (orange) –experimental (blue) of pressure (MPa) on the mandrel during winding (time in minute)

Thanks to the refined model which takes into account artifacts, the simulation is able to capture the winding stage as well as the magnitude of contact stress relaxation during the heat-up portion of the cure cycle.

In comparison when winding with dry tow, pressure increases until reaching an asymptote and no pressure relaxation is observed. For these experimental conditions, the asymptote is reached around 20 layers (Fig. 7). This is well predicted by theory [8].

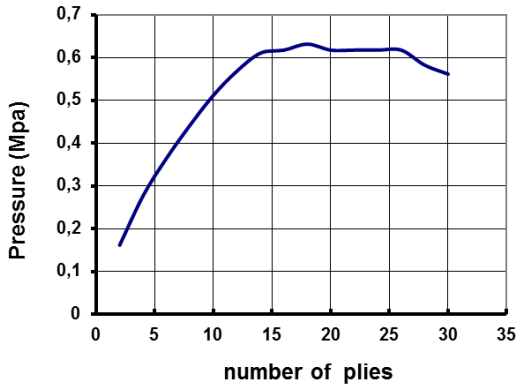

Figure 7: Pressure evolution onto the mandrel with dry IM carbon fiber (winding tension 22N)

5 SIMULATION OF THE PRE-GELATION STATE

5.1 Theory

As discussed earlier, viscous flow of resin and consolidation of fibers are the dominant mechanisms in the pre-gelation regime. The same COMPRO flow-compaction model that was used for winding simulation was continued to simulate the consolidation due to expansion of mandrel up to gelation regime.

5.2 Comparison between simulation and experimental results

The curve in Fig. 8 synthesizes the 3 regimes which characterize the winding process. The gelation is reached during the second heating-up.
During the pre-gelation regime, the pressure on the mandrel doesn't increase significantly and never excess the maximum pressure reached during winding. In fact we observe for both winding tensions, the pressure increases to an asymptote value.

The model developed for winding phase is also able to capture the evolution of pressure on the mandrel during the pre-gelation phase for both winding tension. The computed pressure is higher than experimental value but relaxation of the pressure is quite well simulated when the viscosity reaches its lowest values during the first temperature hold (see Fig. 9).

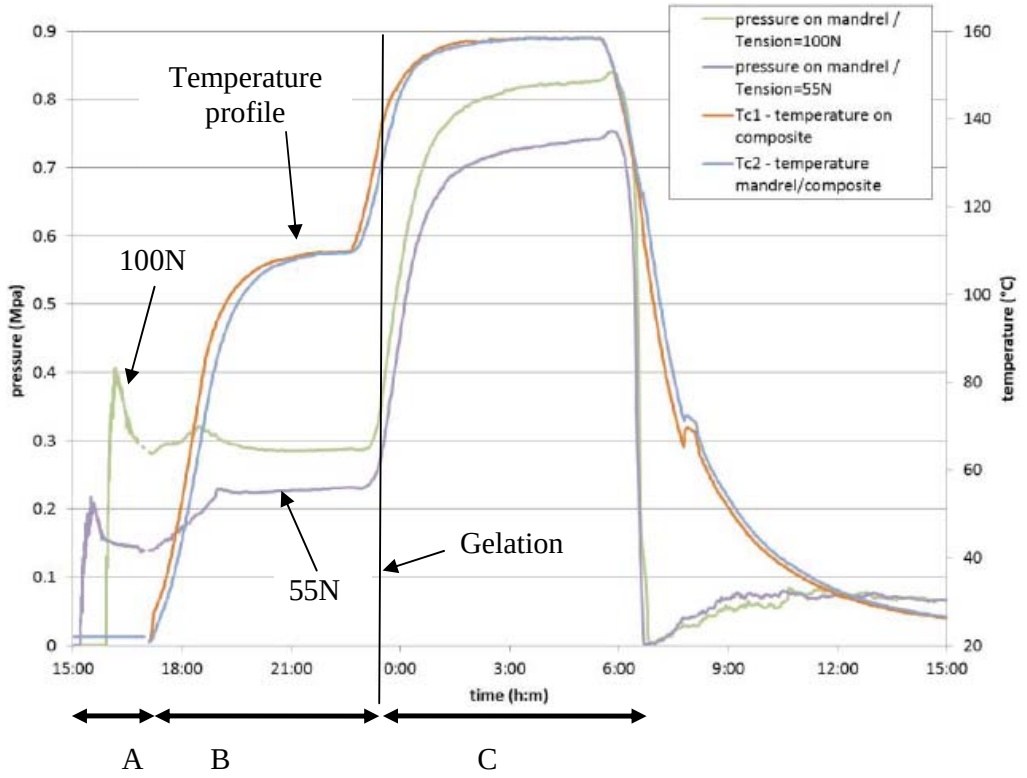

Figure 8: Evolution of the pressure (MPa) on aluminium mandrel for 55N and 100N winding tension - A) Winding; B) pre-gelation; C) post-gelation regime

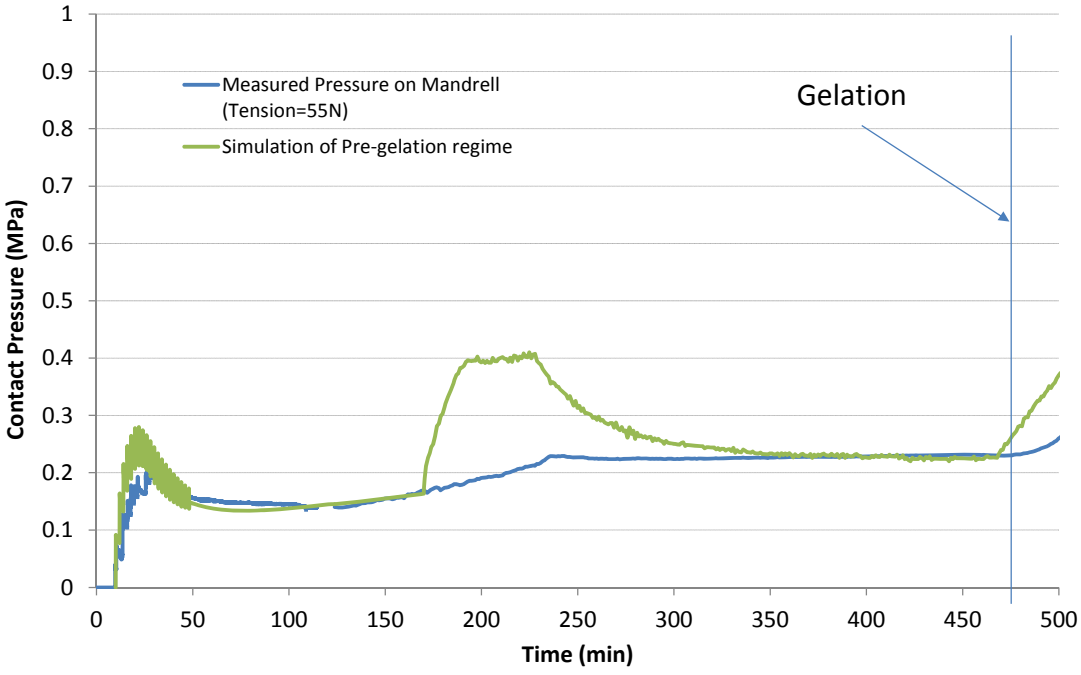

Figure 9: Simulation of the pressure (MPa) on aluminium mandrel in winding and pre-gelation regimes (A) and (B)

6 SIMULATION OF THE POST-GELATION STATE

6.1 Theory

After gelation, the simulation is carried on using Cure Hardening Instantaneously Linear Elastic (CHILE) approach. This approach was originally introduced by Johnston et al [9]. This model that is widely used in composites process simulation, expresses resin modulus as function of temperature and degree of cure. Due to its inherent assumptions, CHILE model is suitable for cure cycles in which resin does not experience devitrification and stress relaxation.

The incremental model is written as follows:

$$d\sigma = C : (d\varepsilon - CTE.dT + CCS.dX) \tag{3}$$

The stiffness matrix C depends on temperature (T) and degree of cure (X) parameters but also with τ (characteristic time of cross linking).

To capture a smooth transition between pre-gelation and post-gelation simulation, stresses induced at the end of pre-gelation consolidation simulation were mapped as initial stresses into the post-gelation simulation (see Fig. 10).

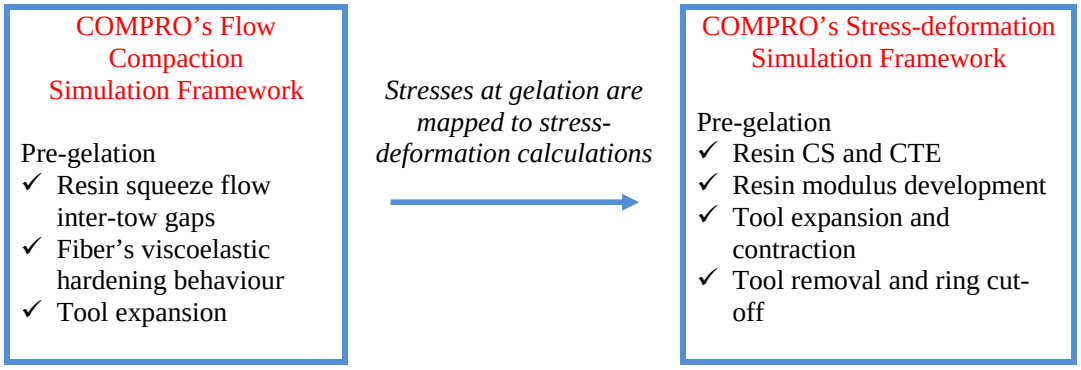

Figure 10: Pre-gelation and post-gelation simulation frameworks and stress mapping at gelation

6.2 Comparison between simulation and experimental results

Fig. 11 shows the predicted pressure on aluminium mandrel surface in both pre-gelation and post-gelation regimes. As it can be seen in this figure, mapping of stresses has resulted in a smooth transition between consolidation and cure simulations.

Simulation results show separation of mandrel from the composite during cooldown stage. This was also observed in the experiments as the mandrel was easily removed from the composite due to the separation.

Comparing FE results with measured pressures presented in Fig. 8, it can be seen that FE model has over-predicted the mandrel pressure by a factor of 2. This discrepancy can be attributed to both FE model, as well as accuracy of pressure sensors in high temperature regime.

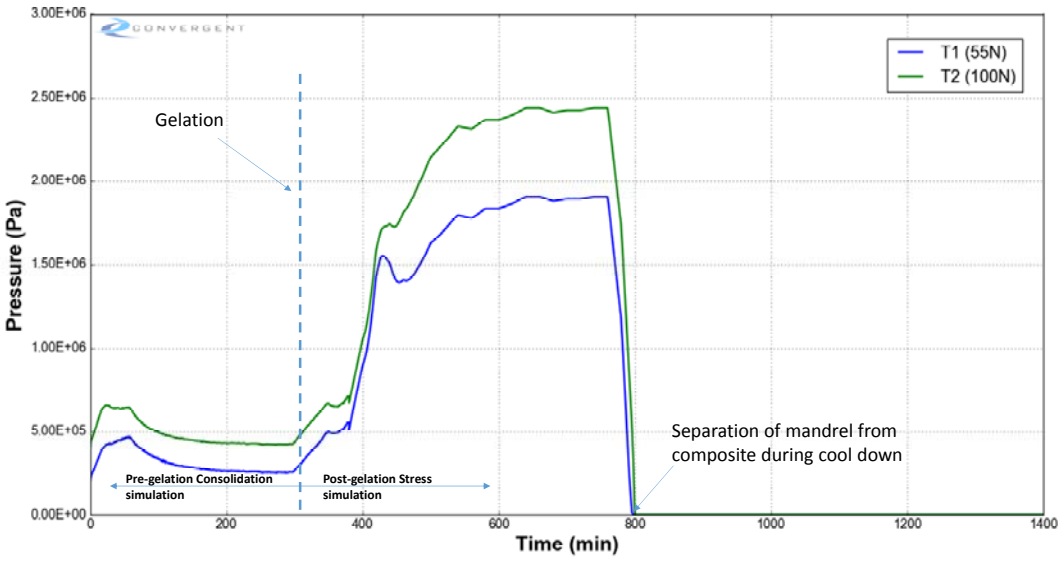

C

Figure 11: Simulation of the pressure on aluminium mandrel in post-gelation phase (C)

Samples are then cut to measure the spring-in angles (Fig. 12). Table 2 shows the predicted spring-in angles versus experimentally measured values. The experimental measurements show the change of tow tension from 55N to 100N has resulted in about 11% increase in spring-in. In FE prediction, similar trend is captured but the increase in the calculated spring-in is about 5.2% (see Table 2).

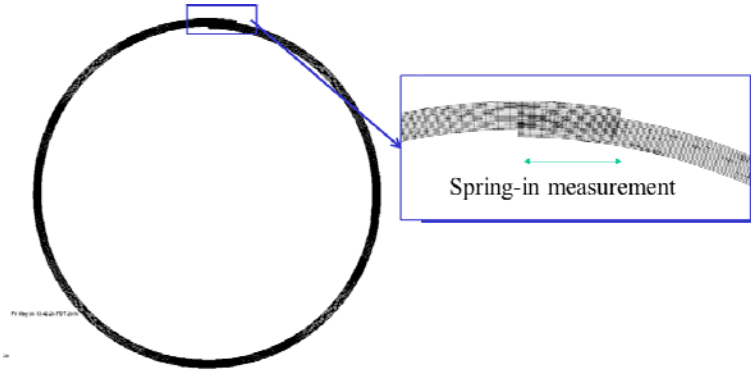

Figure 12: Predicted spring-in angles after cutting of the ring.

Tow tension	Predicted Spring-in	Experimentally measured spring-in
55N	27 mm	35mm
100N	28 mm	39mm

Table 2: Comparison of experimental and simulated spring-in effect with Aluminum alloy – influence of the tow tension

Experimentally we have measured the evolution of fiber volume fraction via image analysis of polished sample cut from the ring. Fig. 13 shows the significant difference of compaction between inner and outer layers of the ring.

It can be seen that there is a general trend of increase in volume fraction moving towards the inner layers which is due to better compaction of the inner layers.

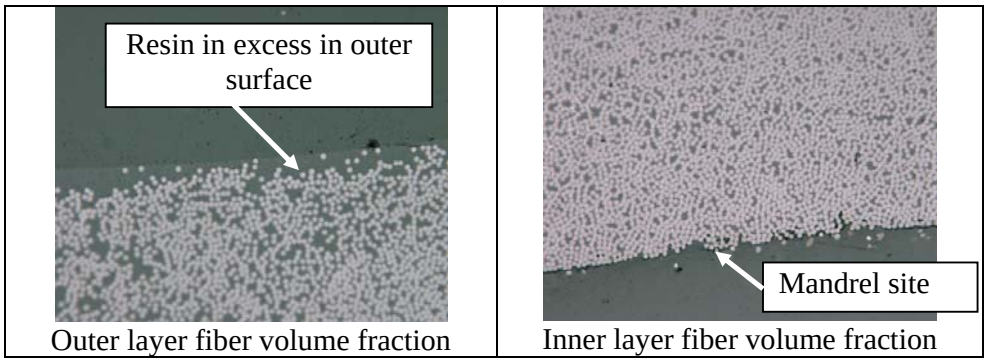

Figure 13: Photomicrograph of fiber volume fraction in $[90]_{20}$ ring

The predicted trend agrees with the experimental observation with a slight excess of resin on the outer surface (see Fig. 14 a). The experimental result doesn't fit exactly the simulation (see Fig 14 b). It can be attributed to both model and methodology used to quantify fiber volume fraction. The discretization mesh of image analysis is not directly linked with ply thickness.

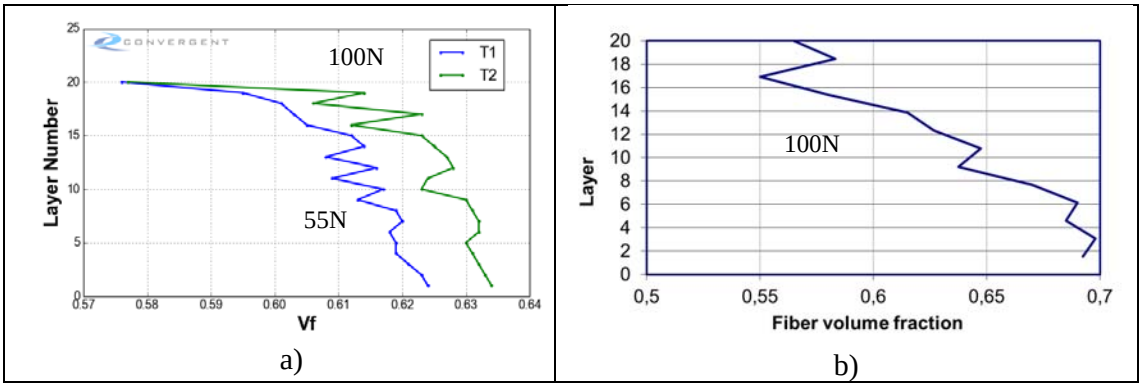

Figure 14: Comparison between simulation a) and experimental measures b) of fiber volume fraction (Vf) throughout $[90]_{20}$ ring thickness

7 DISCUSSION

Complementary investigations have been carried out with the objective to evaluate the sensitivity of some other process parameters. Spring-in measurement has been done with $[90]_{20}$ rings manufactured in the same conditions but with steel mandrel (see Table 3).

Tow tension (N)	Mandrel type	Thickness of the ring after curing (mm)	Spring-in (mm)
50	Steel	7,8	14
100	Steel	7,3	19
55	Aluminum	7,2	35
100	Aluminum	6,8	39

Table 3: Influence of winding tension and type of mandrel on the amplitude of spring-in effect

As expected a lower coefficient of thermal expansion of the mandrel generates less spring-in effect for both winding tensions. Coherent results are also acquired with the variation of the thickness of the rings after curing with respect to winding tension and mandrel thermal property.

Sensitivity of resin properties as resin shrinkage and resin CTE have been investigated by simulation. Results reported in Table 4 are compared to the reference which is the $[90]_{20}$ ring manufactured with aluminum mandrel but without winding tension.

Sensitivity analysis has also been studying by considering the effect of the cure temperature profile. According to Fig.8, a slight gradient of temperature throughout the thickness (9°C maxi) has been noticed. We also investigated the influence of the dwell time of the first hold temperature with the objective to reach gelation during this step (see Table 4).

Tow Tension (N)	Resin Cure Shrinkage	Resin CTE	Tool CTE (m/m°C)	Other parameter	Spring-in trend
0	Included	Included	2.36E-05		1
0	Not included	Included	2.36E-05		-32%
0	Included	Not included	2.36E-05		-11%
0	Included	Included	0.0		-37%
0	Included	Included	3.00E-05		+13%
0	Included	Included	2.36E-05	With curing temperature gradient	-4%
0	Included	Included	2.36E-05	With gelation reach at the first hold	-28%

Table 4: Simulation of the spring-in variation with some process parameters

The following conclusions can be made from these simulations.

- ✓ The major contribution in spring effect is brought by resin cure shrinkage and mandrel thermal expansion; higher shrinkage rate and higher mandrel CTE cause higher residual stresses.
- ✓ Thermal gradient (the outer layer being hotter than layer in contact with mandrel) has low influence in spring-in.
- ✓ A significant reduction of spring-in can be achieved if gelation occurs during the first temperature hold.

If the CTE of the mandrel is quite well known, the uncertainty of resin shrinkage is much higher. The difficulty is to measure resin cure shrinkage without taking into account the change of resin coefficient of thermal expansion from rubbery to glassy state. This difficulty is in principle overcome with DMA method performed by CONVERGENT on bi-material test sample at different isothermal conditions. Nevertheless fidelity of the resin cure shrinkage, deduced from these tests via a micromechanical model is questionable in rubbery regime. This is due to the low transverse modulus of pre-impregnated carbon fiber in this regime. Therefore complementary tests should be performed with another method as gravimetric method based on Archimedean principle or TMA tests allowing to obtain the independent CTE and cure shrinkage values of the resin.

8 CONCLUSION

This study in winding process simulation has allowed to consolidate the methodology followed by Airbus Safran Launchers where the application of Manufacturing Process Simulation can be achieved, if simple tools are available to support process trials, if commercialized Manufacturing Process Simulation tools with standardized test methods for material input data are available and if both manufacturing and design competences are gathered.

From academic point of view, model can be improved if there is a phenomenon that is missing or not properly represented in the simulation but the refinement of the model needs more complex tests.

Before improving model, higher fidelity characterization could be done to achieve better confidence in FE calculations. Increasing number of tests covering several batches of material is suitable but a particular focus must be done in a better characterization of resin cure shrinkage which is a major contributor of spring-in.

REFERENCES

[1] Tzeng Jerome, A model of the winding and curing processes for filament wound composites, *Virginia Polytechnic Institute and State University*, Ph.D, 1988

[2] Soo-Yong Lee and George S Springer “Filament Winding Cylinders: I. Process Model” *Journal of Composites Materials*, Vol. **24** –December 1990 1270-1298

[3] S.R. White, H.T. Hahn, Process modelling of composite materials: Residual stress development during cure, Part I. Model Formulation : *Journal of Composite Materials*, Vol. **26** No 16/1992

[4] D. Cohen, Influence of filament winding parameters on composite vessel quality and strength, *Composites, 1997: part A 28A* (1997) 1035-1047

[5] H.T. Hahn and S.S.Lee « The stress development during filament winding of thick cylinders » *Department of Engineering Science and Mechanics The Pennsylvania State University , report n° 92-25663*, 1992

[6] P Hubert, R Vazari & A Poursartip “ A two-dimensional flow model for the process simulation of complex shape composites laminates” *International Journal for Numerical Method in Engineering* , **44**, 1-26 (1999)

[7] M. Haghshenas, M. R. Vaziri and A. Poursartip, “Integrating the simulation of flow and stress development during processing of thermoset matrix composites” *proceedings of ICCM17,* Edinburgh, Scotland, (2009).

[8] H.T Hahn, E.A. Kempner and J. Slaughter “ The effects of processing and constituent materials on compressive strength of thick composite laminates”, *Mechanical, Aerospace and Nuclear Engineering Department, UCLA*, report 93-26049, 1993

[9] A. Johnston, R. Vaziri and A. Poursartip. A Plane Strain Model for Process-Induced Deformation of Laminated Composite Structures. *Journal of Composite Materials* 2001; **35**(16):1435-1469.